WATER SURFACE CURRENTS, SHORT GRAVITY–CAPILLARY WAVES AND RADAR BACKSCATTER

BY SERHAD S. ATAKTÜRK AND KRISTINA B. KATSAROS

Department of Atmospheric Sciences,
University of Washington, AK–40
Seattle, Washington 98195

Presented at *Air–Sea Interface Symposium, Radio and Acoustic Sensing, Turbulence and Wave Dynamics,* Marseille, France, June 24–30, 1993.

In *The Air–Sea Interface*, M.A. Donelan, W.H. Hui and W.J. Plant, Eds., The University of Toronto Press, Toronto, 1994.

WATER SURFACE CURRENTS, SHORT GRAVITY–CAPILLARY WAVES AND RADAR BACKSCATTER

Serhad S. Ataktürk and Kristina B. Katsaros

Department of Atmospheric Sciences, University of Washington,
Seattle, Washington 98195.

ABSTRACT

Despite their importance for air–sea interaction and microwave remote sensing of the ocean surface, intrinsic properties of short gravity–capillary waves are not well established. This is largely due to water surface currents and their effects on the direct measurements of wave parameters conducted at a fixed point. Frequencies of small scale waves propagating on a surface which itself is in motion, are subject to Doppler shifts. Hence, the high frequency tail of the wave spectra obtained from such temporal observations is smeared. Conversion of this smeared measured–frequency spectra to intrinsic–frequency (or wavenumber) spectra requires corrections for the Doppler shifts. Such attempts in the past have not been very successful in particular when field data were used. This becomes evident if the amplitude modulation of short waves by underlying long waves is considered. Microwave radar studies show that the amplitude of a short wave component attains its maximum value near the crests and its minimum in the troughs of the long waves. Doppler–shifted wave data yield similar results but much larger in modulation magnitude, as expected. In general, Doppler shift corrections reduce the modulation magnitude. Overcorrection may result in a negligible modulation or even in a strong modulation with the maximum amplitude in the wave troughs. The latter situation is clearly contradictory to our visual observations as well as the radar results and imply that the advection by currents is overestimated. In this study, a differential–advection approach is used in which small scale waves are advected by the currents evaluated not at the free surface, but at a depth proportional to their wavelengths. Applicability of this approach is verified by the excellent agreement in phase and magnitude of short–wave modulation between results based on radar and on wave–gauge measurements conducted on a lake.

INTRODUCTION

Spatial measurements can yield directly the wavenumber spectrum of short gravity–capillary waves which is the key quantity in characterization of waves and microwave remote sensing of the ocean surface. Spatial measurements are difficult to obtain, so attempts have been made to determine the wavenumber spectrum from the frequency spectrum of wave height or slope observed at a fixed point in the laboratory (Sinitsyn *et al*, 1973; Reece, 1978) or in the field (Evans and Shemdin, 1980; Ataktürk, 1984; Stolte, 1984, 1989; Richter and Rosenthal, 1986; Ataktürk and Katsaros, 1987). The approach requires relating the wavenumber and the frequency of wave components via a dispersion relation. In the presence of long waves and surface currents, the dispersion relation for short waves is greatly altered (Kitaigorodskii *et al*, 1975) and the problem is complicated.

In a Eulerian frame of reference, the observed frequency of a short wave depends on its translational speed as it passes by the probe. If a wave component is travelling at its phase speed, $\boldsymbol{c}(\omega)=\omega/\boldsymbol{k}$, then the observed frequency is its intrinsic frequency, ω, which is related to the wavenumber, $\boldsymbol{k}$, via the dispersion relation, $\omega=(g+Tk/\varrho_w)k^2$, where g is the gravitational acceleration, ϱ_w is the density of water, and T is the surface tension. If the waves are riding on a surface which itself is in motion, then their observed translational speed is the sum of their phase speed and the component of the surface current, $\boldsymbol{U}_s$, in the direction of wave propagation specified by the unit vector $\boldsymbol{k}/k$. In this case, the observed frequency is $\sigma=\omega+\boldsymbol{k}\cdot\boldsymbol{U}_s=\omega+kU_s\cos\phi$.

In *The Air–Sea Interface*, M.A. Donelan, W.H. Hui and W.J. Plant, Eds., The University of Toronto Press, Toronto, 1994.

The wave field considered in this study is generated purely by the local winds over the limited fetch of a lake, where tide and swell are not present. Then, the surface velocity can be described as, $\mathbf{U}_s(t) = \mathbf{U}_\zeta + \mathbf{U}_{St} + \mathbf{U}_w$, where the three terms on the right hand side are the horizontal orbital velocity of the long gravity waves, wave–induced mass transport (Stokes drift), and wind–induced surface drift, respectively. Then, the relation between the frequency of encounter, σ, and the intrinsic frequency, ω, becomes; $\sigma=\omega+\boldsymbol{k}\cdot(\mathbf{U}_\zeta+\mathbf{U}_{St}+\mathbf{U}_w)$, which is an explicit form of the Doppler frequency shift. The dispersion relation appropriate for this case may be described as before with g replaced by a modified gravitational acceleration, g', which includes the additional effects caused by the underlying long waves (Garrett and Smith, 1976; Phillips, 1981; Longuet–Higgins, 1985).

In the past, Doppler shift corrections have been made using the currents evaluated at the free surface. In the present study it is shown that this approach may lead to unrealistic results. Therefore, an alternative approach in which the short waves are assumed to be advected by the current evaluated at a depth proportional to their wavelengths is tried. The appropriateness of the latter approach is verified by experimental results.

EXPERIMENTAL SET–UP AND INITIAL DATA PROCESSING

The field data used in this study were collected during the summers of 1986 through 1989 at Sand Point, Lake Washington, Seattle. The research facility is operated by the University of Washington, Department of Atmospheric Sciences. It consists of a mast located 15 *m* offshore, a hut situated on a beached barge and a floating dock between the mast and the land. On the beach, one end of the dock is mounted on a rotating base so that the other end can swing between the barge and the mast. In order to prevent interference with the measurements, during data acquisition the dock is secured along the shore away from the mast. A data link between the instruments on the mast and the data acquisition system in the hut is supplied by underwater cables.

Ideal experimental conditions at this site are achieved during northerly winds when the fetch over the lake reaches a maximum of about 7 *km*. The location offers a unique opportunity to study surface waves generated by the local wind on a natural body of water under a variety of environmental conditions without the complexities that may arise from the presence of swell or tidal currents. The water depth, D, by the mast is approximately 4*m* and increases rapidly further offshore. We estimate the degree of reflection of the gravity waves from the inclined beach to be 5% or less (Miche, 1951). When $kD>\pi/2$, the waves are said to be in deep water (Phillips, 1977, p. 37). This corresponds to $\lambda=2\pi/k<16\ m$, where λ is the wavelength. Since this condition was met in all cases (typically $\lambda\cong 5\ m$ for the dominant gravity waves), the location can be considered as representative of deep water.

During the experiments, the following variables (Table 1) were directly measured or observed using the indicated instrumentation. Radar measurements were conducted by the University of Kansas group and are described by Salam *et al* (1991). Details of our work including various corrections to measured signals and data processing techniques are provided by Ataktürk (1984, 1991) and Ataktürk and Katsaros (1987, 1989).

Table 1: List of directly observed variables and instrumentation used. Radar measurements were conducted by the University of Kansas.

Wave height	Resistance wire gauge
Wind components	K–Gill anemometer
Air temperature (dry & wet bulb)	Thermocouples
Water temperature	Thermistors
Visible surface features	Video camera
Electromagnetic backscatter	Microwave radar

In *The Air–Sea Interface*, M.A. Donelan, W.H. Hui and W.J. Plant, Eds., The University of Toronto Press, Toronto, 1994.

Initial data processing involved the following calculations. Surface fluxes of momentum, sensible heat and latent heat were determined by the eddy correlation method for every 17–minute segment of data. This provided us with the surface friction velocity, u_*, atmospheric stratification parameter, z/L, and surface roughness length parameter, z_o. Further, a digital linear–phase, band–pass filter was applied to the wave height time series, $\zeta(t)$, to separate its high–frequency (3–17Hz) part, $\zeta'(t)$. A Fast Fourier Transform algorithm and a sliding window of 0.5 second long were applied to $\zeta'(t)$ to create a time series of the measured frequency spectra, $E(\sigma)$ with a sampling rate of 8Hz.

Surface currents were not directly measured but estimated from u_* or $\zeta(t)$ via a linear wave theory. For a monochromatic wave train, these relationships can be described by

$$\zeta(t) = A\cos(kx - \omega t)\ ;\quad U_\zeta = \zeta\omega\, e^{kz}\ ;\quad U_{St} = \omega k\, A^2 e^{2kz};\quad U_w = 0.60\, u_* \qquad (1)$$

In the case of field data, contributions from wave components with frequencies up to three times the peak frequency were included. In previous studies, U_{St} has been ignored and U_w has been approximated by 3% of U_{10}, wind speed adjusted to 10m height and neutral atmospheric stratification.

Doppler frequency shifts were corrected in the frequency domain according to the transformation

$$E(\sigma)\, d\sigma = E(\omega)\, d\omega = E(k)\, dk \qquad (2)$$

by using two different methods to estimate the effective surface currents. In the first method, which has been used by all investigators sited at the beginning of this section, surface currents were calculated as above and the effective current was taken as that at the free surface, z=0. The second approach was different in the sense that the effective wind drift was taken as that at a depth of z=–0.044λ (Plant and Wright, 1977, 1980)

$$U_w\,(z = -0.044\lambda) = U_w(z=0) - \left(\frac{\varrho_a}{\varrho_w}\right)^{1/2} \frac{u_*}{\varkappa}\left(\frac{z_{ow} + z}{z_{ow}}\right) \qquad (3)$$

where z_{ow} is roughness length parameter for water, ϱ_a is the density of air, and $\varkappa$ is the von Kármán constant (also see, Stewart and Joy, 1974; Donelan, 1978; Donelan *et al*, 1985; Smith, 1990). It should be noted that in determining this particular depth, Plant and Wright (1977, 1980) approximated z_{ow} with z_o, surface roughness length parameter. The same approximation was also used here.

Evaluating Equations 1 and 3 requires knowledge of u_* and z_o. Although these variables were available to us through the atmospheric turbulence measurements, they can not be determined with adequate accuracy over short periods of time due to sampling variability. To overcome this difficulty, a method was developed to obtain an estimate of z_o from the measured wave height spectra such that

$$z_{o\zeta} = 7.2\text{x}10^{-3}\, \zeta_{rms} \left(\frac{\alpha_m}{0.006}\right)^{2.1} \qquad (4)$$

where ζ_{rms} is the root–mean–square wave height, and α_m is the *measured* equilibrium range parameter (mean spectral amplitude in the range $1.5<\omega/\omega_p<3.5$ with ω_p being the peak frequency; for details see, Ataktürk [1991]). Success of this approach is illustrated in Figures 1 and 2.

The tool selected for the final evaluation of the experimental results from this study is the modulation transfer function (MTF). Following the definitions by Plant (1989), modulation of a variable $x(t)$ by the underlying long waves, and the coherence function, γ^2, for this modulation were calculated from

$$m(f) = \frac{X(f)\ \zeta^*(f)}{k\overline{X}\ |\zeta(f)|^2}\ ;\qquad \gamma 2(f) = \frac{|X(f)\ \zeta^*(f)|^2}{|X(f)|^2\ \ |\zeta(f)|^2} \qquad (5)$$

where $X(f)$ and $\varsigma(f)$ are the Fourier transforms of $x(t)$ and $\varsigma(t)$, $\overline{X}$ is the mean of $x(t)$, and * denotes the complex conjugate. Since $m(f)$ is a complex quantity, its full description requires knowledge of both magnitude and phase. By convention, phase is zero at the long wave crest, and positive ahead of it.

In *The Air–Sea Interface*, M.A. Donelan, W.H. Hui and W.J. Plant, Eds., The University of Toronto Press, Toronto, 1994.

EXPERIMENTAL RESULTS

Radars operating in *C* (6 *GHz*), *X* (11 *GHz*) and *Ka* (34 *GHz*) bands provided information on MTF for Bragg wavelengths about 3 *cm* or shorter (for results on *C* and *X* bands, see Salam et al, 1991). On the other hand, quality of the wave data for wavelengths shorter than about 5 *cm* were questionable. Therefore, in evaluation of the results we considered other radar studies as well, specifically Wright *et al* (1980) and Plant *et al* (1983) which provided information in the wavelength ranges of both our radar and wave data . For the purpose of this study, the following summary of the radar results is sufficient. In the wind speed range of 3 to 7 *m/s* and for dominant waves with a frequency of 0.5 *Hz*, the magnitude of MTF varies approximately between 5 and 10 decreasing with increasing wind speed. Dependence on wind speed is weaker for longer Bragg waves. Maximum modulation occurs somewhere between the crest and 30 degrees ahead of it. Coherence between the radar return and wave height is strong (γ^2=0.6) near the frequency of the dominant waves but rapidly diminishes away from the spectral peak. There is little difference between *C* and *X* bands. It should be kept in mind that MTF obtained from radar measurements has three components: hydrodynamic, tilt and range modulation, or $m(f) = m' - it + r$, where $i = (-1)^{1/2}$. For our conditions where the radars were mounted about 5 *m* above the surface with incident angle varying between 30 and 60° , *r* is negligible and $|t| \simeq 4$ (Plant, 1990). Then, the magnitude of the hydrodynamic modulation, m', which is the quantity provided by analysis using the wave data is expected to vary between 3 and 9.

Results from wave data were obtained using the time series of wave height and short wave spectra in Equation 5. In Figure 3, the rows correspond to the cases of measured spectra, intrinsic spectra with Doppler correction according to Equation 1 (Method A), and intrinsic spectra with Doppler correction according to Equations 1 and 3 (Method B). The first column is the maximum coherence squared (at the frequency of dominant waves) for each run. The dashed line indicates the level, γ^2=0.1 below which we assumed that the two signals were incoherent. Such points were excluded from MTF analysis. The second column is the phase of MTF for all data points with $\gamma^2 \geq 0.1$. Mean magnitude of MTF for these points are shown in the third column. The vertical bars indicate ±1 standard deviation. Features to be noted in this figure can be summarized as follows.

MTF magnitude determined from measured spectra is at first fairly uniform across the wavelength range, then it slightly increases for $\lambda \lesssim 15$ *cm*. This is in accordance with the concept that Doppler frequency shift poses more serious problems at higher frequencies. Rapid decrease for $\lambda < 5$ *cm* is suspected to be due to noise in the data. The observed increase with increasing wind speed is contrary to radar results, and is due to the Doppler frequency shift becoming stronger with the growth of long waves. As indicated by the MTF phase, maximum modulation occurs at the wave crests.

When Doppler shift corrections were made using the currents evaluated at the free surface (Method A), resulting MTF had no resemblance to those of the radars except at the longer wavelengths, where Doppler shift effects are not significant. In the midrange, both the coherence and modulation diminished. Although they reach generally expected values for $\lambda \lesssim 15$ *cm*, in this region the MTF phase becomes ±180 implying that short waves attain their maximum amplitudes in the long wave troughs. This is completely against the radar results as well as visual observations, and can be explained by overcorrection for Doppler shifts.

The results based on the approach that short waves are advected by the current at a depth proportional to their wavelengths (Method B), are similar to those of radar studies except for $\lambda < 5$ *cm* where further considerations are needed. Dependence of MTF magnitude on wind speed becomes significant at shorter wavelengths where the MTF magnitude decreases with wind. Observed MTF phase is about zero indicating that short waves attain their maximum amplitudes near the crests of long waves.

In *The Air–Sea Interface*, M.A. Donelan, W.H. Hui and W.J. Plant, Eds., The University of Toronto Press, Toronto, 1994.

CONCLUSIONS AND DISCUSSIONS

Generally it has been assumed that the short gravity–capillary waves are advected by the currents evaluated at the free surface. In this study it is shown that the effective advection velocity is rather the current evaluated at a depth which is proportional to the lengths of the short waves considered. This conclusion is based on the comparisons of the hydrodynamic modulation of short wave amplitudes determined through wave and radar measurements conducted on a lake. Even when this differential advection approach is used, some conflicts were observed between the radar and wave results for wavelengths about 5 *cm* and shorter. This is possibly due to an assumption made in Doppler shift corrections that the wind, surface currents and waves of all scales propagate in the same direction. For our experimental site, this assumption is quite appropriate except for small scale waves. Currently, we are experimenting with the design of an array of wire staffs to obtain the directional wavenumber spectrum at these wavelengths.

ACKNOWLEDGMENTS

The authors would like to thank the University of Kansas Center for Research, Inc. for providing the radar data. This research was supported by the National Aeronautics and Space Administration under Grant NAGW–1322.

REFERENCES

Ataktürk S.S., 1984: Intrinsic frequency spectra of small scale wave amplitude measured in a lake. M. Sc. Thesis, University of Washington, AK–40, Seattle, WA, 98195, 96 pp.

Ataktürk, S.S., 1991: Characterization of roughness elements on a water surface. Ph. D. Dissertation, University of Washington, AK–40, Seattle, WA, 98195, 196 pp.

Ataktürk, S.S. and K.B. Katsaros, 1987: Intrinsic frequency spectra of short gravity–capillary waves obtained from temporal measurements of wave height on a lake. *J. Geophys. Res.*, **92**, 5131–5141.

Ataktürk, S.S. and K.B. Katsaros, 1989: The K–Gill: A twin propeller–vane anemometer for measurements of atmospheric turbulence. *J. Atmos. Ocean. Tech.*, **6**, 509–515.

DeCosmo, J., 1991: Air–sea exchange of momentum, heat and water vapor over whitecap sea states. Ph. D. Dissertation, University of Washington, AK–40, Seattle, WA, 98195, 213 pp.

Donelan, M.A., 1978: Whitecaps and momentum transfer. In *Turbulent Fluxes Through the Sea Surface, Wave Dynamics and Prediction*, A. Favre and K. Hasselmann, Eds., Plenum Press, New York, pp. 273–287.

Donelan, M.A., J. Hamilton and W.H. Hui, 1985: Directional spectra of wind–generated waves. *Phil. Trans. R. Soc. Lond.*, **A 315**, 509–562.

Evans, D.D. and O.H. Shemdin, 1980: An investigation of the modulation of capillary and short gravity waves in the open ocean. *J. Geophys. Res.*, **85**, 5019–5024.

Garrett, C. and J. Smith, 1976: On the interaction between long and short surface waves. *J. Phys. Oceanogr.*, **6**, 925–930.

Kitaigorodskii, S.A., V.A. Krasitskii and M.M. Zavlavskii, 1975: On Phillips' theory of equilibrium range on the spectra of wind–generated gravity waves. *J. Phys. Oceanogr.*, **5**, 410–420.

Longuet–Higgins, M.S., 1985: Accelerations in steep gravity waves. *J. Phys. Oceanogr.*, **15**, 1570–1579.

Miche, M., 1951: Action of the swell. *Ann. Ponts Chaussees*, **121**, 285–319.

Phillips, O.M., 1977: *The Dynamics of the Upper Ocean.* Cambridge University Press, 336 pp.

Phillips, O.M., 1981: The dispersion of short wavelets in the presence of a dominant long wave. *J. Fluid Mech.*, **107**, 465–485.

Plant, W.J., 1989: The modulation transfer function: concept and applications. In *Radar Scattering from Modulated* Wind Waves, G.J. Komen and W.A. Oost, Eds., Kluwer Academic Publishers, 155–172.

Plant, W.J., W.C. Keller and A. Cross, 1983: Parametric dependence of ocean wave–radar transfer functions. *J. Geophys. Res.*, **88**, 9747–9756.

Plant, W.J. and J.W. Wright, 1977: Growth and equilibrium of short gravity waves in a wind–wave tank. *J. Fluid Mech.*, **82**, 767–793.

Plant, W.J. and J.W. Wright, 1980: Phase speeds of upwind and downwind traveling short gravity waves. *J. Geophys. Res.*, **85**, 3304–3310.

Reece, A.M., 1978: Modulation of short waves by long waves. *Bound. Layer Meteorol.*, **13**, 203–214.

Richter, K. and W. Rosenthal, 1986: Energy distribution of waves above 1 Hz on long wind waves. In *Wave Dynamics and Radio Probing of the Ocean Surface*, O.M. Phillips and K. Hasselmann, Eds., Plenum Press, New York, pp. 75–93.

Salam, A., D. Bush, S. Gogineni and A. Zaide, 1991: Preliminary Report: Fundamental Studies of Radar Scattering from Water Surfaces, The Lake Washington Experiment. *RSL Technical Report 7970–2*, Radar Systems and Remote Sensing Laboratory, University of Kansas Center for Research, Inc., 2291 Irving Hill Road, Lawrence, KA. 66045–2969.

Sinitsyn, Y.A., I.A. Leykin and A.D. Rozenberg, 1973:The space–time characteristics of ripple in the presence of long waves. *Izv. Acad. Sci. U.S.S.R., Atmos. Ocean. Phys.*, Engl. Transl., **9**, 511–519.

Smith, J.A., 1990: Modulation of short wind waves by long waves. In *Surface Waves and Fluxes: Volume 1– Current Theory*, G. Geernaert and W.J. Plant, Eds., Kluwer Academic Press, Dordrecht, The Netherlands, pp. 247–284.

Stewart, R.H. and J.W. Joy , 1974: HF radio measurements of surface currents. *Deep Sea Res.*, **21**, 1039–1049.

Stolte, S., 1984: Modulation of short waves by long wind waves and wind. Ph. D. Dissertation, University of Hamburg, Germany, 199 pp.

Stolte, S., 1989: Short wave modulation and breaking, experimental results. In *Radar Scattering from Modulated* Wind Waves, G.J. Komen and W.A. Oost, Eds., Kluwer Academic Publishers, Norwell, MA., pp. 201–210.

Wright, J.W., W.J. Plant, W.C. Keller and W.L. Jones, 1980: Ocean wave radar modulation transfer functions from the West Coast Experiment. *J. Geophys. Res.*, **85**, 4957–4966.

FIGURE LEGENDS

Figure 1: Comparison of the surface roughness lengths determined from: (o) wave measurements on Lake Washington; (–) a model particularly for low winds (Lui, Katsaros and Businger, 1979); and, (*) atmospheric turbulent measurements during *HEXMAX* (DeCosmo, 1991). Dashed line is a fit to *HEXMAX* results.

Figure 2: Comparison of neutral drag coefficients determined from: (o) wave and (+) atmospheric turbulent measurements on Lake Washington; and, (*) atmospheric turbulent measurements during *HEXMAX* (DeCosmo, 1991). Dashed line is a fit to *HEXMAX* results.

Figure 3: Magnitude and phase of MTF and coherence squared obtained from analysis of the wave data against the short–wave length. The rows (from top to bottom) correspond to the cases of measured spectra, intrinsic spectra with Doppler correction according to Equation 1, and intrinsic spectra with Doppler correction according to Equations 1 and 3. Method–B, bottom row, is preferred. Symbols in figures indicate different ranges of wind speeds in *m/s* such that (3–4: ...+...), (4–5: – –x– –) and (5–7: —o—). The dashed line in the plots of coherence squared indicates a value of 0.1.

In *The Air–Sea Interface*, M.A. Donelan, W.H. Hui and W.J. Plant, Eds., The University of Toronto Press, Toronto, 1994.

FIG. 1

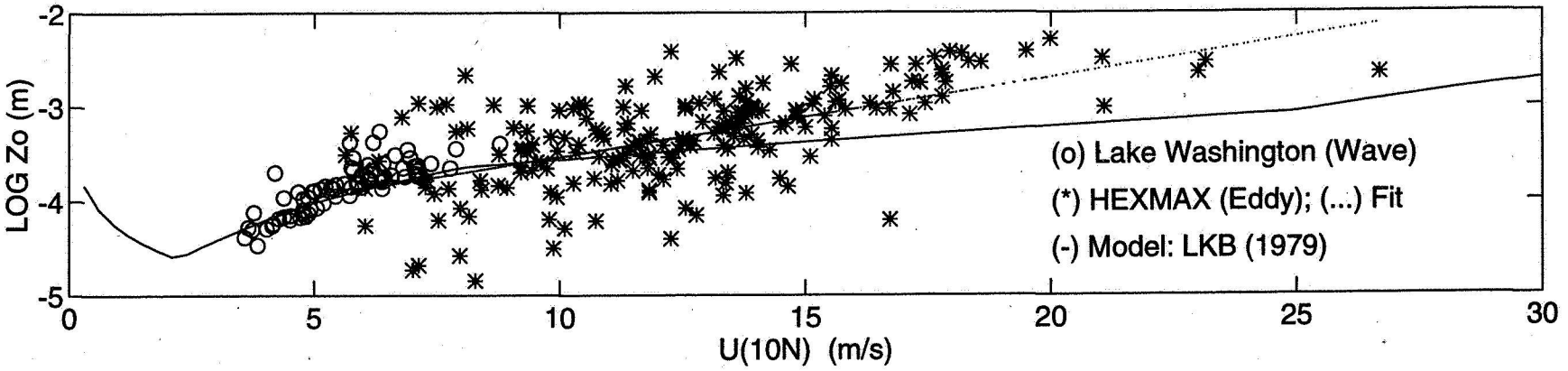
LOG Zo (m)
-2
-3
-4
-5
0
5
10
15
20
25
30
U(10N) (m/s)
(o) Lake Washington (Wave)
(*) HEXMAX (Eddy); (...) Fit
(-) Model: LKB (1979)

FIG. 2

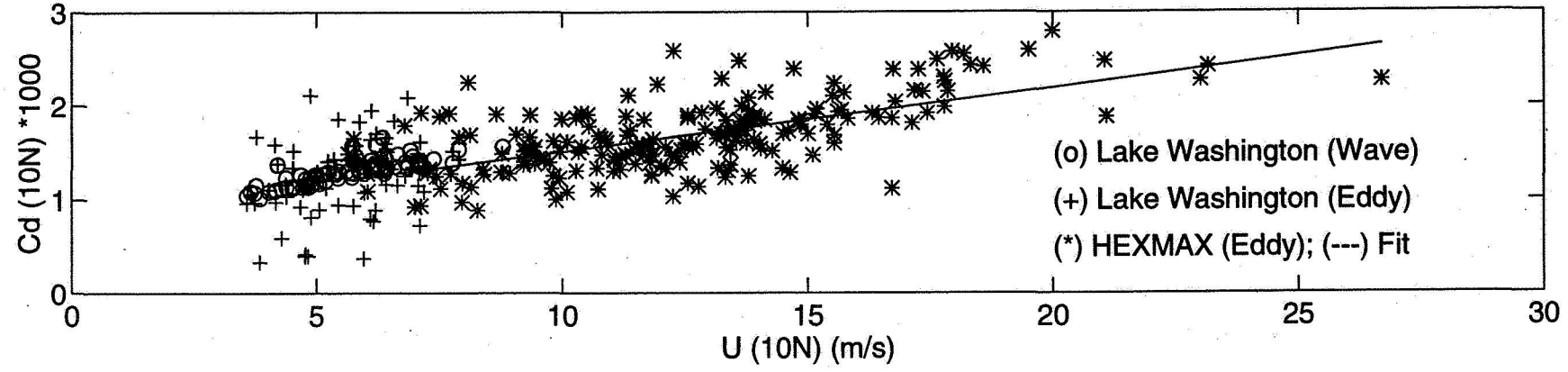
Cd (10N) *1000
3
2
1
0
0
5
10
15
20
25
30
U (10N) (m/s)
(o) Lake Washington (Wave)
(+) Lake Washington (Eddy)
(*) HEXMAX (Eddy); (---) Fit

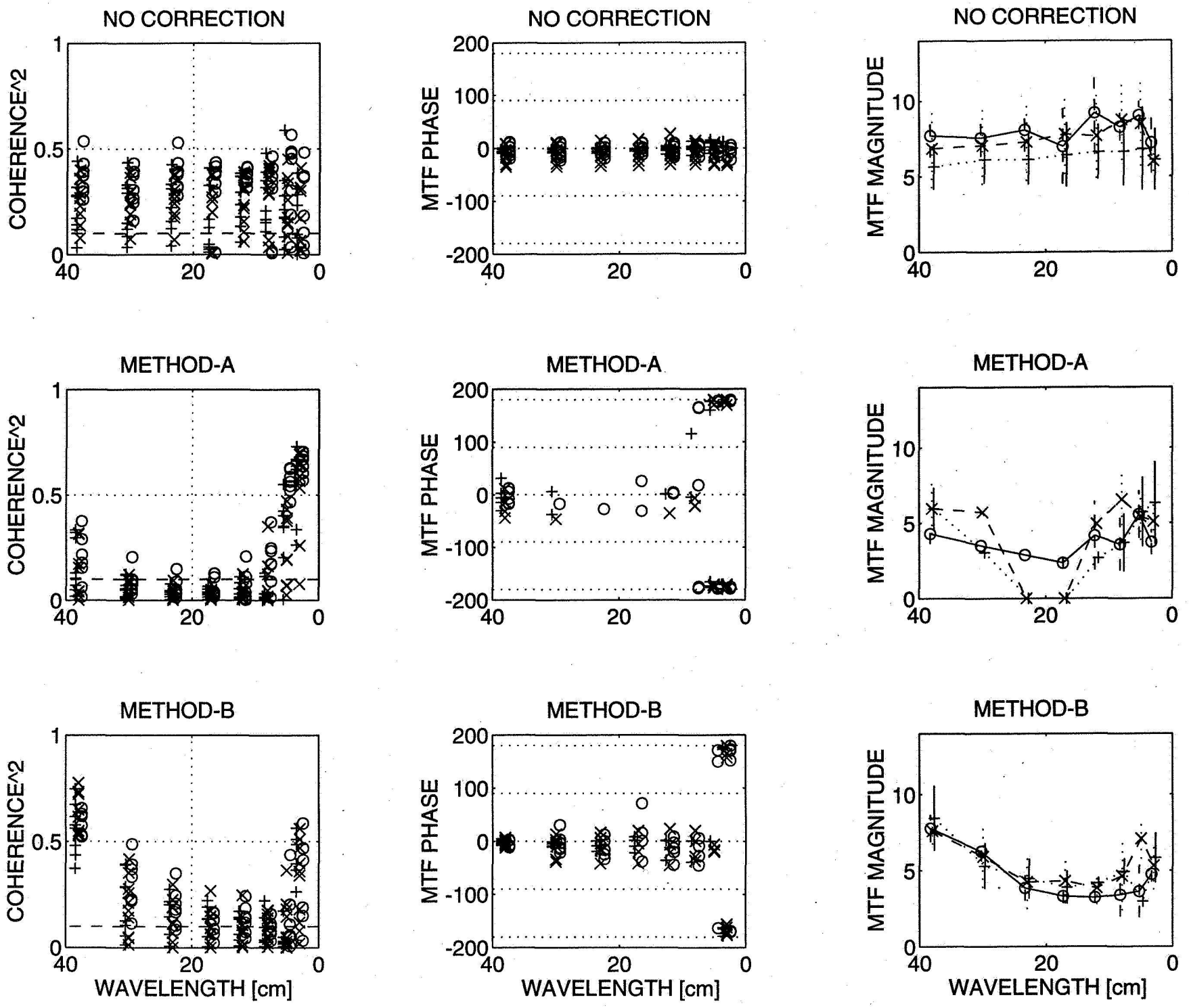
NO CORRECTION
COHERENCE^2
MTF PHASE
MTF MAGNITUDE
METHOD-A
METHOD-B
WAVELENGTH [cm]

FIG. 3